JACS
JOURNAL OF THE AMERICAN CHEMICAL SOCIETY
Article
pubs.acs.org/JACS

Mechanism of Alcohol Oxidation Mediated by Copper(II) and Nitroxyl Radicals

Bradford L. Ryland, Scott D. McCann, Thomas C. Brunold, and Shannon S. Stahl*

Department of Chemistry, University of Wisconsin—Madison, 1101 University Avenue, Madison, Wisconsin 53706, United States

Supporting Information

ABSTRACT: 2,2′-Bipyridine-ligated copper complexes, in combination with TEMPO (2,2,6,6-tetramethylpiperidine-*N*-oxyl), are highly effective catalysts for aerobic alcohol oxidation. Considerable uncertainty and debate exist over the mechanism of alcohol oxidation mediated by Cu^{II} and TEMPO. Here, we report experimental and density functional theory (DFT) computational studies that distinguish among numerous previously proposed mechanistic pathways. Oxidation of various classes of radical-probe substrates shows that long-lived radicals are not formed in the reaction. DFT computational studies support this conclusion. A bimolecular pathway involving hydrogen-atom-transfer from a Cu^{II}–alkoxide to a nitroxyl radical is higher in energy than hydrogen transfer from a Cu^{II}–alkoxide to a coordinated nitroxyl species. The data presented here reconcile a collection of diverse and seemingly contradictory experimental and computational data reported previously in the literature. The resulting Oppenauer-like reaction pathway further explains experimental trends in the relative reactivity of different classes of alcohols (benzylic versus aliphatic and primary versus secondary), as well as the different reactivity observed between TEMPO and bicyclic nitroxyls, such as ABNO (ABNO = 9-azabicyclo[3.3.1]nonane *N*-oxyl).

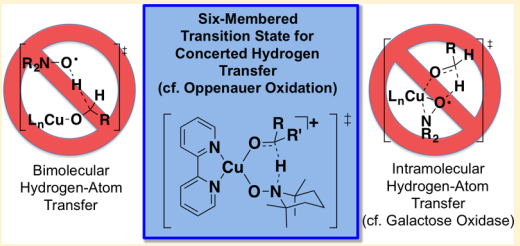

INTRODUCTION

Aerobic alcohol oxidation mediated by homogeneous copper/nitroxyl cocatalysts has been the subject of extensive recent investigation.[1] These catalyst systems achieve some of the most efficient, selective, and functional-group-tolerant means to oxidize alcohols to aldehydes and ketones. They often use ambient air as the source of oxidant and achieve complete conversion within 1 h at room temperature. Two highly effective complementary catalyst systems are shown in Scheme 1. The Cu/TEMPO (TEMPO = 2,2,6,6-tetramethylpiperidine-*N*-oxyl) catalyst system (Scheme 1A),[2,3] which features a Cu^{I} source such as $[Cu(MeCN)_4]OTf$ in combination with 2,2′-bipyridine (bpy), TEMPO, and *N*-methylimidazole (NMI), exhibits very high chemoselectivity for oxidation of primary alcohols. For example, the steric sensitivity of this catalyst system enables selective oxidation of unprotected diols, wherein only the least sterically hindered primary alcohol is oxidized. The Cu/ABNO (ABNO = 9-azabicyclo[3.3.1]nonane *N*-oxyl) catalyst system[4,5] (Scheme 1B) is similar, but uses the less sterically hindered bicyclic ABNO cocatalyst, and it enables rapid oxidation of both primary and secondary alcohols, including molecules containing diverse functional groups.

The synthetic utility of Cu/nitroxyl catalyst systems has led to considerable interest in the mechanism of these reactions. An early study[3a] emphasized the relationship between Cu/TEMPO and other TEMPO-catalyzed alcohol oxidation reactions that proceed via an oxoammonium/hydroxylamine cycle.[6] The latter reactions are effective with a variety of terminal oxidants, such as NaOCl, Br_2 and $PhI(OAc)_2$ (Scheme 2). An O_2-coupled Cu^{II}/Cu^{I} redox cycle was proposed to oxidize TEMPOH to the oxoammonium species in the Cu/TEMPO-catalyzed

Scheme 1. Cu/TEMPO and Cu/ABNO Aerobic Alcohol Oxidation Catalyst Systems

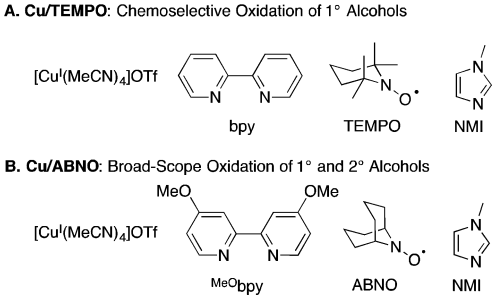

Scheme 2. Oxoammonium/Hydroxylamine Mechanism for Alcohol Oxidation with Diverse Terminal Oxidants

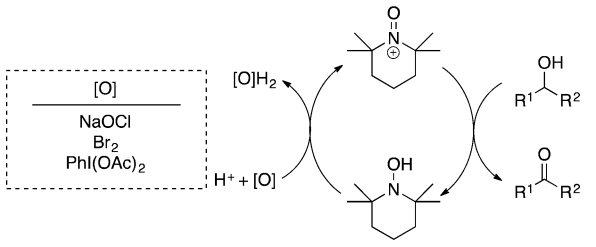

Received: July 11, 2014
Published: August 4, 2014

dx.doi.org/10.1021/ja5070137 | J. Am. Chem. Soc. 2014, 136, 12166–12173

reactions;[3a] however, subsequent studies by us[7] and others[3c,8] demonstrated that a different mechanism is involved in these reactions. Electrochemical studies showed that the Cu^{II} reduction potential is not high enough to generate the oxoammonium species under the reaction conditions,[7] and kinetic isotope effects (KIEs) revealed that an oxoammonium reagent and the reactive oxidant in Cu/TEMPO-catalyzed oxidation reactions exhibit different intrinsic isotope effects for alcohol oxidation.[7a,8] Extensive additional kinetic and in situ spectroscopic studies support the (simplified) catalytic mechanism shown in Scheme 3.[7] Molecular oxygen oxidizes

Scheme 3. Catalytic Mechanism for Cu/TEMPO-Catalyzed Aerobic Alcohol Oxidation

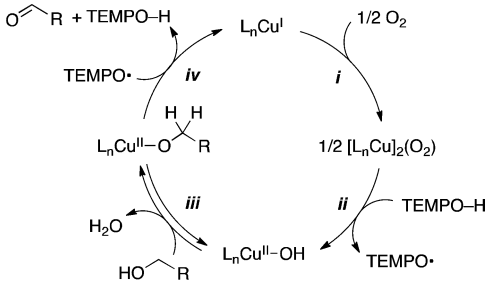

Cu^I and the hydroxylamine (TEMPOH) to a Cu^{II}–OH species and TEMPO radical in steps i and ii, and Cu^{II}–OH and TEMPO then mediate oxidation of the alcohol to the aldehyde (steps iii and iv, Scheme 3).

The mechanism in Scheme 3 explains the kinetic differences observed between activated and unactivated alcohols. Benzylic, allylic, and other activated alcohols are oxidized rapidly in step iv and feature turnover-limiting oxidation of Cu^I by O_2 (step i). Unactivated aliphatic alcohols react more slowly and exhibit turnover-limiting cleavage of the C–H bond (step iv). The latter reactions exhibit a saturation dependence on [alcohol] and a first-order dependence on [TEMPO], consistent with the sequence shown in steps iii and iv. Insights such as these provided a foundation for the discovery of the Cu/ABNO catalyst system (cf. Scheme 1B),[4] which exhibits faster rates and broader scope, but many fundamental questions about the mechanism of alcohol oxidation by Cu^{II} and nitroxyl remain unanswered.

The mechanism of Cu^{II}/nitroxyl-mediated alcohol oxidation has been the subject of considerable speculation and debate. Three of the most prominent mechanistic proposals are depicted in Scheme 4. In 1966, Brackman and Gaasbeek reported the first example of Cu/nitroxyl-catalyzed alcohol oxidation in the oxidation of methanol with phenanthroline/Cu^{II} species and di-*tert*-butylnitroxyl.[9] They observed inhibition of the reaction under more basic conditions and proposed that the nitroxyl radical abstracts a hydrogen atom from a neutral methanol ligand coordinated to Cu^{II} (Scheme 4A). Sheldon and co-workers highlighted similarities between Cu/nitroxyl catalysts and galactose oxidase,[8a] an enzyme that features an active site with a Cu^{II}-coordinated phenoxyl radical from a modified tyrosine side chain (Figure 1). The oxidation of different benzylic alcohols by a Cu/nitroxyl catalyst system was shown to exhibit KIEs and Hammett correlations similar to those reported for galactose oxidase, and the authors proposed a galactose oxidase-like mechanism involving hydrogen atom transfer to an η^2-coordinated nitroxyl radical (Scheme 4B; cf.

Scheme 4. Mechanistic Proposals for Cu^{II}/Nitroxyl-Mediated Alcohol Oxidation

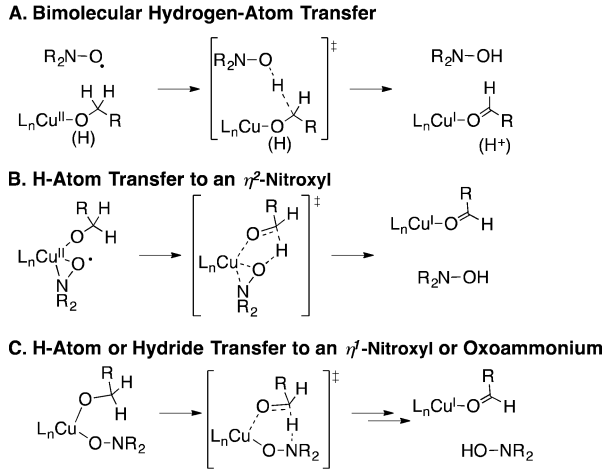

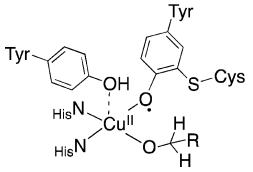

Figure 1. Active site structure of galactose oxidase.

Figure 1). This proposal finds additional support from precedents for Cu^{II} complexes bearing η^1- and η^2-coordinated nitroxyl ligands.[10] Finally, density functional theory (DFT) computational studies have been used to probe the nature of hydrogen transfer from an alkoxide ligand to a coordinated nitroxyl.[11,12] Compelling studies by Baerends and co-workers identified a low-energy pathway involving hydrogen transfer from the alkoxide to an η^1-coordinated nitroxyl (Scheme 4C).[11]

Each of the mechanisms in Scheme 4 is potentially consistent with experimental data; however, recent spectroscopic and kinetic studies of Cu/TEMPO-catalyzed alcohol oxidation did not provide evidence for a Cu/TEMPO adduct under catalytic conditions.[3c,7,13] In addition, a first-order kinetic dependence on [Cu] and [TEMPO] observed in the oxidation of aliphatic alcohols seems most consistent with a bimolecular mechanism analogous to that in Scheme 4A. The computationally derived mechanism in Scheme 4C[11] was published before the recent experimental studies and cannot be compared directly to the experimental results (e.g., activation barriers) because these studies started from a $[(bpy)Cu^{II}(alkoxide)(nitroxyl)]^+$ complex that is not the resting state of the catalyst.

Here, we report experimental and computational data that directly assess the mechanisms in Scheme 4. Several radical-probe substrates have been used to probe whether discrete radical intermediates are involved in alcohol oxidation (cf. Scheme 4A,B). DFT computational studies of (bpy)Cu/TEMPO- and (bpy)Cu/ABNO-mediated alcohol oxidation have been carried out, starting from a $[(bpy)Cu(OH)(NMI)]^+$ species that has been proposed as the catalyst resting state. Inclusion of the full ligand and nitroxyl (TEMPO and ABNO) structures enables quantitative comparison of the computational results with experimental data, including relative reactivity trends between benzylic/aliphatic and primary/secondary alcohols and between TEMPO/ABNO nitroxyl cocatalysts. The collective results reconcile previously reported

dx.doi.org/10.1021/ja5070137 | J. Am. Chem. Soc. 2014, 136, 12166–12173

experimental and computational data and support a closed-shell two-electron hydrogen-transfer pathway most closely resembling that in Scheme 4C. The results further explain the reactivity and chemoselectivity differences observed with TEMPO and ABNO cocatalysts.

RESULTS AND DISCUSSION

Oxidation of Radical Probe Substrates. Galactose oxidase-mediated alcohol oxidation is proposed to proceed via a ketyl radical intermediate.[14] This conclusion is supported by results with radical-probe substrates, such as cyclopropyl carbinol derivatives. Cyclobutanol is another probe molecule used to distinguish between one- and two-electron alcohol oxidation pathways.[15−21] For example, oxidation of cyclobutanol by permanganate leads to ring-opened products,[20] while oxidation by perruthenate affords only cyclobutanone.[21] These observations support stepwise one-electron and concerted two-electron pathways, respectively, with these reagents.

Five different radical-probe substrates were subjected to the previously reported Cu/TEMPO aerobic alcohol oxidation conditions (Table 1). In all cases, efficient oxidation was

Table 1. Cu/TEMPO-Catalyzed Aerobic Oxidation of Radical-Probe Substrates

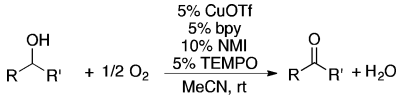

Entry	Substrate	Carbonyl Product	Yield (%)[a]	Expected Radical Rearrangement Product (Not observed)
1	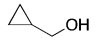		96	
2			95	
3[b]	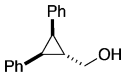	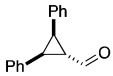	94	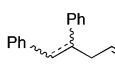
4	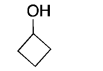		90	
5	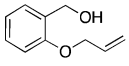	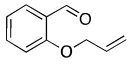	>99	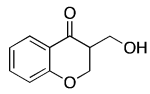

[a]Yield determined by ^{1}H NMR spectroscopy (int. std. = trimethoxybenzene). [b]No *trans*−*cis* isomerization observed.

observed to afford the unrearranged aldehyde or ketone in nearly quantitative yield, based on ^{1}H NMR analysis. The cyclopropyl carbinol derivatives (entries 1−3) show no ring-opening to the homoallylic products.[22,23] Cyclopropyl radical ring-opening is known to be a reversible process,[24] but the lack of *trans*−*cis* isomerization of 2,3-*trans*,*trans*-diphenyl-cyclopropanemethanol (entry 3) indicates that a ring-opening/ring-closure equilibrium does not occur. Cyclobutanol affords only cyclobutanone (entry 4), and no cyclizaton of the benzylic alcohol is observed under the reaction conditions (entry 5). The last substrate has been shown to rearrange via a 6-*exo*-*trig*-cyclization to a chromanone derivative when subjected to alcohol oxidation conditions that proceed via one-electron steps.[25]

To our knowledge, the rate constants for rearrangement of the ketyl radical anions derived from these substrates have not been determined, but rate constants for the corresponding neutral radicals are $>10^8$ s^{-1}.[22,26] This consideration, together with evidence for radical intermediates when these substrates have been used with galactose oxidase and other oxidants, suggests that discrete radical intermediates are not involved in Cu/nitroxyl-mediated alcohol oxidation.

Experimental Benchmarks for Computational Studies. With these results in hand, we turned our attention to DFT computational studies designed to enable direct comparison with experimental data. The following experimental observations provide important benchmarks to assess the validity of computed reaction pathways:

1. Cu/TEMPO-catalyzed alcohol oxidation reactions exhibit the following relative reactivity trends: primary benzylic alcohols > primary aliphatic alcohols ≫ secondary aliphatic alcohols.

2. The experimental activation barrier for benzyl alcohol oxidation is <15 kcal/mol (i.e., less than that associated with the turnover-frequency,[27] which is limited by aerobic oxidation of Cu^I as the turnover-limiting step) and is 15−16 kcal/mol for the primary aliphatic alcohol cyclohexanemethanol, which was used in previous mechanistic studies.[7]

3. Spectroscopic studies provide no direct evidence for a Cu/TEMPO adduct under the catalytic reaction conditions, and the oxidation of the aliphatic primary alcohols exhibits a first-order kinetic dependence on [Cu] and [TEMPO] and a saturation dependence on [alcohol].[7] These data demonstrate that the catalyst resting state cannot be a Cu/TEMPO adduct. Electron paramagnetic resonance (EPR) spectroscopic analysis of the catalytic reaction mixture supports the presence a mononuclear bpy-ligated Cu^{II} species. A (bpy)Cu^{II}−hydroxide resting state, such as $[(bpy)Cu(OH)(NMI)]^+$, is most consistent with the data.

4. Alcohol oxidation does not proceed via a discrete radical intermediate.

5. Alcohol oxidation by the Cu/ABNO catalyst system proceeds with a much lower barrier than Cu/TEMPO, and Cu/ABNO mediates facile oxidation of secondary aliphatic alcohols.

We used the OPBE density functional in our DFT computational studies, following the lead of Baerends et al.[11] Comparative calculations were carried out with the B3LYP and M06-L functionals, but both of these functionals led to poor agreement with experimental data.[28] The experimental solvent, acetonitrile, was modeled using the SMD continuum solvation model.

Formation of Cu−Alkoxides Species. The experimental data implicate an equilibrium between (bpy)Cu^{II}−OH and (bpy)Cu^{II}−OCH_2R species (cf. benchmark #3 in the previous section). Several four- and five-coordinate structures of this type were evaluated, with NMI and/or acetonitrile ancillary ligands, and the most stable species was found to be $[(bpy)Cu^{II}(OH)(NMI)]^+$ (Figure 2). Equilibria for formation of Cu^{II}−alkoxide species derived from benzyl alcohol, and 1- and 2-propanol (as representative benzylic, primary aliphatic and secondary aliphatic substrates) were calculated. In each case, the energy of the Cu^{II}−alkoxide is higher than that of the Cu^{II}−hydroxide, with relative stabilities of Cu^{II}−alkoxides $\mathbf{2}^{\mathbf{Bn}}$, $\mathbf{2}^{\mathbf{n Pr}}$, and $\mathbf{2}^{\mathbf{i Pr}}$ showing a qualitative correlation with the alcohol pK_a values: benzyl alcohol > 1-propanol > 2-propanol.[29,30] These Cu^{II}−alkoxide species served as starting points for

dx.doi.org/10.1021/ja5070137 | J. Am. Chem. Soc. 2014, 136, 12166−12173

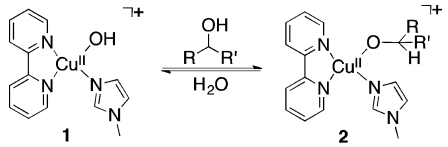

Alcohol	ΔG°
Benzyl Alcohol	0.6
1-Propanol	2.1
2-Propanol	4.2

Figure 2. Equilibrium for formation of Cu–alkoxide species.

assessment of the different oxidation pathways depicted in Scheme 4.

Bimolecular Hydrogen Atom Abstraction Pathway. On the basis of the lack of evidence for TEMPO coordination to (bpy)Cu^{II} and the first-order rate dependence on [Cu] and [TEMPO] (cf. benchmark #3 in the previous section), we previously proposed that alcohol oxidation occurs via bimolecular abstraction of a hydrogen atom from a Cu^{II}–alkoxide by TEMPO.[7a] This reaction was evaluated for various (bpy)Cu^{II}–alkoxide species. The lowest energy pathway for hydrogen-atom transfer was found from $[(bpy)Cu^{II}(OR)(CH_3CN)]^+$ species, which have a slightly higher ground-state energy than the analogous NMI-ligated species (ΔG° < 2 kcal/mol) (Scheme 5). The transition state energies for benzyl, 1-propyl, and 2-propyl alcohol derivatives were all very similar, at 20.6, 21.0, and 21.8 kcal/mol, respectively. The H atom transfer step exhibits a linear C···H···O trajectory, while the geometry of the copper center shifts from square-planar to distorted tetrahedral in the transition state. Transition states with a closed-shell electronic structure are lowest in energy, consistent with the reduction of Cu^{II} to Cu^{I} taking place in concert with the H atom transfer step.

These calculations show that a bimolecular hydrogen-atom transfer process is energetically accessible. It further accounts for the experimental rate law, and the lack of evidence for a radical intermediate can be explained by homolytic C–H cleavage occurring in concert with reduction of Cu^{II} to Cu^{I}, thereby avoiding formation of a carbon-centered radical. On the other hand, the calculated barrier for oxidation of benzyl alcohol (20.6 kcal/mol) is substantially higher than the 15 kcal/mol upper limit for this substrate determined experimentally,[27] and the different barriers calculated for primary and secondary alcohols do not account for the dramatic reactivity differences observed with these two classes of alcohols.

Hydrogen Transfer to η^1- and η^2-Coordinated TEMPO Adducts of Copper(II). Reaction pathways involving η^1 and η^2 Cu^{II}–nitroxyl adducts (cf. Scheme 4B,C) provide alternatives to bimolecular hydrogen-atom transfer. An η^2–TEMPO adduct $\mathbf{6}^{n\mathbf{Pr}}$ was identified computationally by replacement of NMI in $[(bpy)Cu(OnPr)(NMI)]^+$ with TEMPO (Figure 3). This

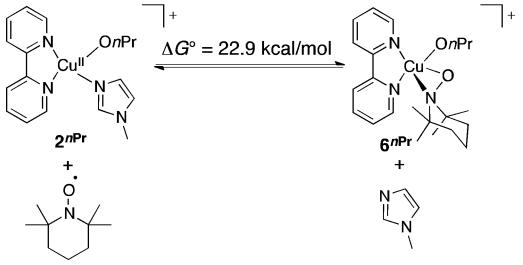

Figure 3. Equilibrium for formation of η^2–nitroxyl complex, $\mathbf{6}^{n\mathbf{Pr}}$.

complex has a closed-shell singlet electronic structure. An attempt to optimize a triplet structure resulted in the dissociation of the TEMPO ligand and optimization of an open-shell singlet produced a closed-shell singlet electronic

Scheme 5. Free Energy Surface for Cu^{II}/TEMPO-Mediated Alcohol Oxidation via Bimolecular Hydrogen Atom Transfer (cf. Scheme 4A)

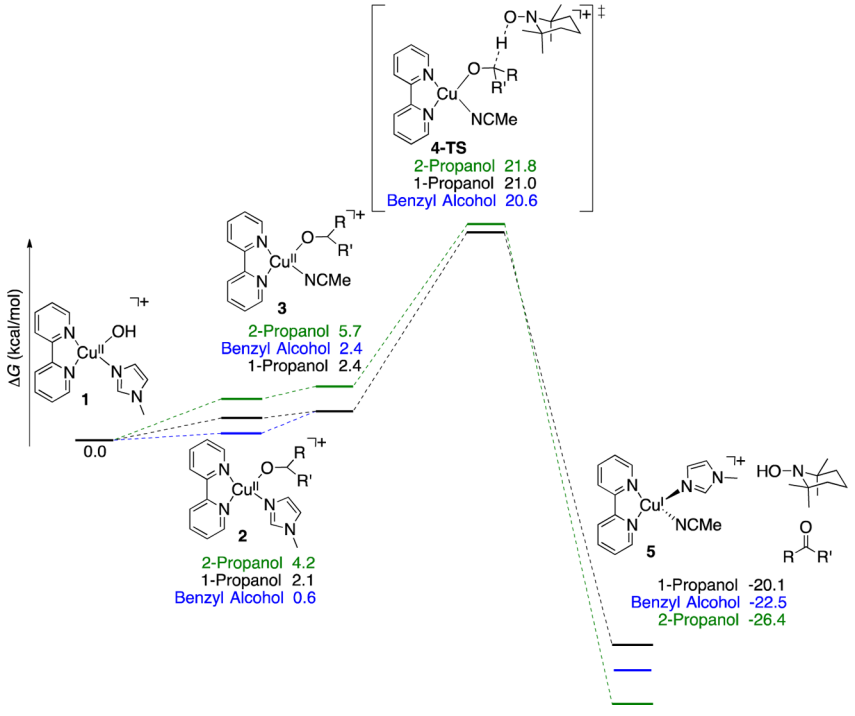

dx.doi.org/10.1021/ja5070137 | J. Am. Chem. Soc. 2014, 136, 12166–12173

structure. The free energy of complex $\mathbf{6}^{n\mathrm{Pr}}$ is 22.9 kcal/mol higher than that of the Cu^{II}–alkoxide complex $\mathbf{2}^{n\mathrm{Pr}}$, (i.e., 25.0 kcal/mol higher than that of the reference Cu^{II}–hydroxide complex **1**), and 4.0 kcal/mol higher than that of the transition state energy for the bimolecular hydrogen atom transfer pathway (cf. Scheme 5). The latter comparison suggests alcohol oxidation does not proceed via an η^2–nitroxyl, since the transition state for H atom transfer would be even higher in energy than $\mathbf{6}^{n\mathrm{Pr}}$.

Coordination of TEMPO as an η^1 adduct is more favorable than as an η^2 adduct (cf. Figures 3 and 4). This complex, $\mathbf{7}^{n\mathrm{Pr}}$, also has a closed-shell singlet electronic structure. Displacement of NMI by TEMPO in Figure 4 remains substantially uphill energetically (+13.6 kcal/mol), but it is significantly lower in energy than the transition state for bimolecular H atom transfer, and this complex was used as a starting point for calculation of a full pathway for alcohol oxidation (Scheme 6).

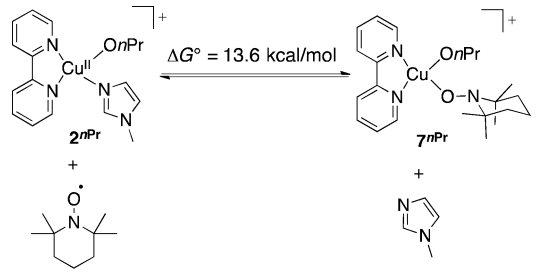

Figure 4. Equilibrium for formation of η^1–nitroxyl complex, $\mathbf{7}^{n\mathrm{Pr}}$.

Different energies are observed for the η^1–TEMPO adducts $\mathbf{7}^{\mathrm{Bn}}$, $\mathbf{7}^{n\mathrm{Pr}}$, and $\mathbf{7}^{i\mathrm{Pr}}$; however, their relative energies are compressed relative to the corresponding NMI adducts $\mathbf{2}^{\mathrm{Bn}}$, $\mathbf{2}^{n\mathrm{Pr}}$, and $\mathbf{2}^{i\mathrm{Pr}}$. The low-energy pathway involves hydrogen transfer from the alkoxide to the unbound nitrogen atom of the η^1–TEMPO ligand via a six-membered transition state (**8-TS**), similar to that identified by Baerends et al.[11] The transition-state energy exhibits a significant dependence on the identity of the alkoxide ligand, with the secondary *i*-propoxide complex having an energy 6.3 kcal/mol higher than that of the primary *n*-propoxide complex (cf. Scheme 6). In all cases, the barrier for hydrogen transfer is small (<5 kcal/mol) from the $[(bpy)Cu(OR)(\eta^1\text{–TEMPO})]^+$ intermediate (**7**), and the overall energy for the oxidation of the synthetically relevant primary alcohols $PhCH_2OH$ and *n*PrOH is <17 kcal/mol relative to the resting state $[(bpy)Cu(OH)(NMI)]^+$ species (**1**).

Overall, this reaction pathway shows excellent agreement with the experimental data. The predicted rates follow the trends observed experimentally: primary benzylic alcohols > primary aliphatic alcohols ≫ secondary aliphatic alcohols. The activation energies of 15.8 and 16.9 kcal/mol calculated for benzyl alcohol and 1-propanol are very close to the ∼15 kcal/mol barrier determined experimentally, and the significantly higher barrier calculated for 2-propanol concurs with the lack of reactivity observed with 2° alcohols under experimental conditions. The concerted hydrogen transfer step in **8-TS** explains the lack of radical rearrangement products observed with the substrates in Table 1.

Our previous kinetic studies of Cu/TEMPO-catalyzed alcohol oxidation[7] showed that the catalytic rate exhibits a first-order dependence on [TEMPO], and EPR spectroscopic analysis of the reaction mixture provided no evidence for TEMPO coordination to $(bpy)Cu^{II}$. These observations led us to propose a bimolecular H atom transfer mechanism for the reaction, similar to the mechanism in Scheme 4A. The results in Scheme 6, however, provide an alternative explanation for the experimental data. The first-order kinetic dependence on [TEMPO] and the lack of experimentally detectable nitroxyl

Scheme 6. Free Energy Surface for Cu^{II}/TEMPO-Mediated Alcohol Oxidation via Hydrogen Transfer to η^1-Bound TEMPO

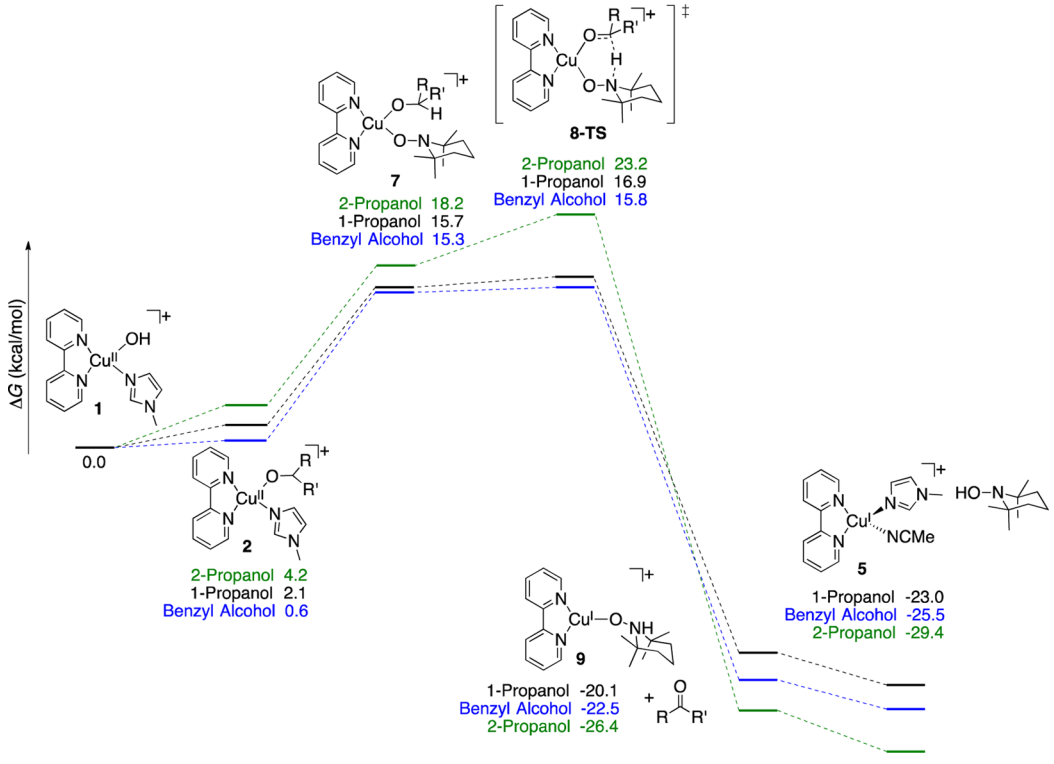

dx.doi.org/10.1021/ja5070137 | J. Am. Chem. Soc. 2014, 136, 12166–12173

Scheme 7. Cu^{II}/ABNO-Mediated Oxidation of 1-Propanol and 2-Propanol

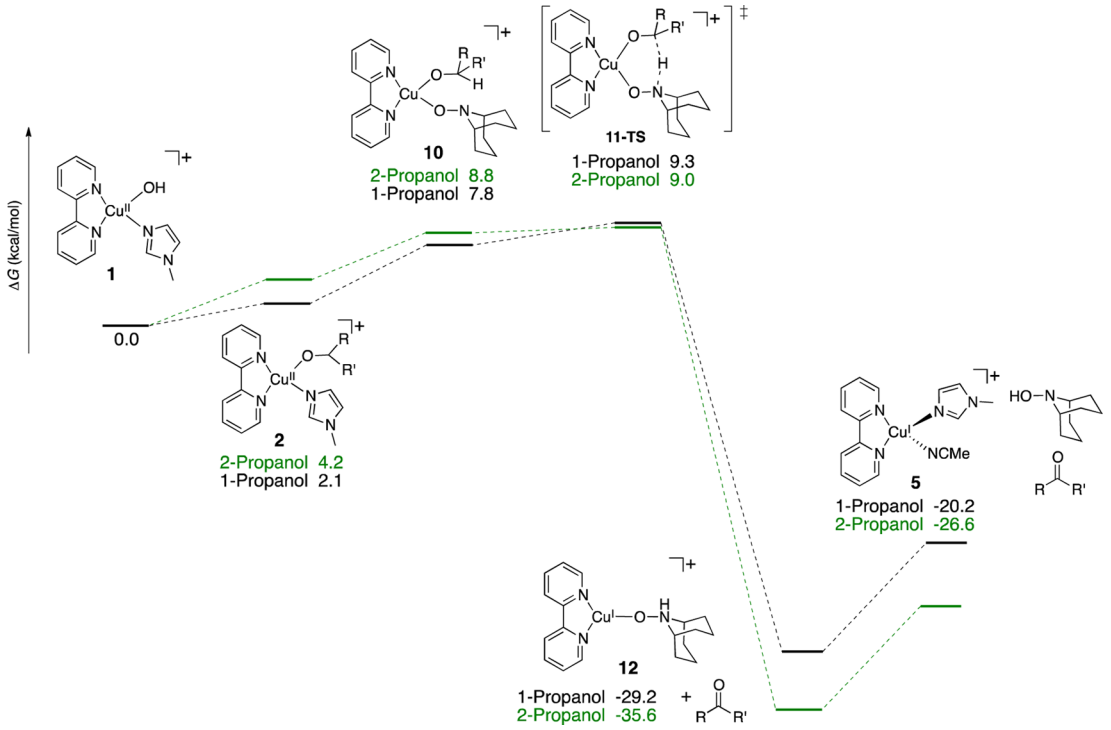

coordination to Cu^{II} can be explained by an unfavorable pre-equilibrium for TEMPO binding to Cu^{II} (cf. Figure 4). A rate law corresponding to the mechanism in Scheme 6 (eq 1; see Supporting Information for derivation of the rate law) is consistent with the first-order dependence on [TEMPO] (as well as the saturation kinetic dependence on $[RCH_2OH]$ and first-order dependence on [Cu], observed experimentally[7]).

$$\frac{d[\text{product}]}{dt} = \frac{K_1 k_2 k_3 [\text{Cu}]_{\text{tot}} [\text{TEMPO}][\text{RCH}_2\text{OH}]}{(k_3 + k_{-2})(1 + K_1[\text{RCH}_2\text{OH}])} \quad (1)$$

Cu^{II}/ABNO-Mediated Alcohol Oxidation. The only experimental result not explained by the data above is the reactivity different between TEMPO and ABNO (see benchmark #5 above). These nitroxyls have very similar redox potentials,[31] but considerably different steric profiles, and the Cu/ABNO catalyst system exhibits significantly higher activity with 1° and 2° aliphatic alcohols. The η^1–nitroxyl pathway in Scheme 6 was re-evaluated with Cu^{II}/ABNO for the oxidation of 1- and 2-propanol (Scheme 7). The ABNO adduct **10** and corresponding hydrogen-transfer transition state **11-TS** exhibit much lower energies than the TEMPO-derived structures. The overall barriers for Cu^{II}/ABNO-mediated oxidation of 1- and 2-propanol are less than 10 kcal/mol, and there is essentially no difference between the barrier for the two different alcohol substrates. Similar results are obtained with AZADO (2-azaadamantane *N*-oxyl), a nitroxyl with electronic and steric profiles similar to ABNO (Supporting Information Figure S2). These results show that steric effects can have a significant influence on the stability of Cu^{II}/nitroxyl adducts and their reactivity toward alcohol oxidation.

Mechanistic Analysis and Comparison to Other Alcohol Oxidation Methods. The experimental and computational studies outlined above clearly distinguish among the mechanisms that have been proposed for Cu/TEMPO-catalyzed alcohol oxidation. The elegant and compelling analogy between Cu/nitroxyl catalyst systems and galactose oxidase is undermined by the lack of evidence for radical intermediates in the Cu/TEMPO reactions (cf. Table 1). The computational results further show that a bimolecular pathway for hydrogen-atom transfer (cf. Schemes 4A and 5), which is conceptually related to the intramolecular hydrogen-atom transfer step proposed for galactose oxidase, has a barrier that is too high in energy to account for the experimental results, and does not reproduce the substrate steric effects observed in the reactions.

On the other hand, the experimental data are fully explained by a mechanism involving concerted hydrogen transfer from an alkoxide ligand to an η^1-coordinated nitroxyl. Structurally characterized Cu–TEMPO complexes have been reported in the literature, including examples with η^1 and η^2 TEMPO coordination modes (Figure 5).[10,32] Each of these complexes is

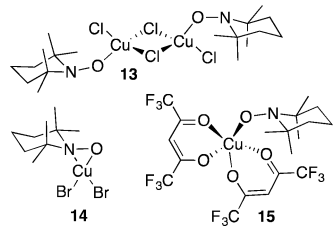

Figure 5. Structurally characterized Cu–nitroxyl complexes.

diamagnetic, consistent with the closed-shell singlet electronic structure of the $[(bpy)Cu(OR)(nitroxyl)]^+$ intermediates **7** and **10** described above (cf. Schemes 6 and 7). The η^2–TEMPO coordination mode is much too high in energy to participate the catalytic reaction (cf. Figure 3 and Scheme 4B), but the η^1 coordination mode is energetically accessible. Nevertheless, coordination of TEMPO as an η^1 adduct is sufficiently uphill energetically that the adduct cannot be detected experimentally.

dx.doi.org/10.1021/ja5070137 | J. Am. Chem. Soc. 2014, 136, 12166–12173

A previous study of the well-defined Cu–TEMPO complexes **13** and **14** (Figure 5) noted that pyridine readily displaces TEMPO from Cu,[10d] so perhaps it is not surprising that TEMPO coordination is disfavored in the presence of bpy and NMI as ancillary ligands.

The six-membered transition state for hydrogen transfer in Schemes 6 and 7 shows considerable resemblance to the transition state for Oppenauer oxidation of alcohols mediated by $Al(iOPr)_3$ (Figure 6).[33] The latter mechanism involves

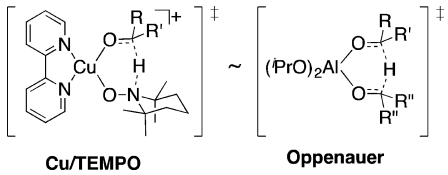

Figure 6. Structural similarity between the transition states for alcohol oxidation in Cu/TEMPO and Oppenauer oxidation methods.

approximately thermoneutral hydrogen transfer from an Al^{III}-bound alkoxide to a coordinated ketone, such as acetone, as a hydrogen acceptor. While the two transition states are structurally similar, Cu^{II}/nitroxyl-mediated alcohol oxidation features a thermodynamic driving force associated with reduction of Cu^{II} and nitroxyl to Cu^{I} and hydroxylamine, and oxidation of Cu^{I} and hyroxylamine by O_2 continuously replenishes the oxidized species (Scheme 3). This driving force in the reaction expands the scope of alcohols that can be oxidized effectively.

Substantial contemporary efforts are focused on replacing noble-metal catalysts with first-row transition metals. One intrinsic challenge in achieving this goal is the tendency of first-row transition metals to undergo one-electron, rather than two-electron, redox steps. The Cu/nitroxyl catalysts show how a first-row transition metal can be combined with a one-electron redox-active organic cocatalyst to achieve a two-electron transformation, and their mechanism may be compared to palladium(II)-catalyzed alcohol oxidation reactions.[34] The latter reactions feature Pd^{II}–alkoxide intermediates that undergo β-hydride elimination via a four-membered transition state (Figure 7). This step is often the turnover-limiting step of the reaction. The six-membered transition state for Cu/nitroxyl-mediated alcohol oxidation should have less strain, which may may account for the lower barrier associated with these reactions.[35] The identification of new catalyst systems that exploit the redox synergy between transition metal and organic cocatalysts represents a promising target for future studies.

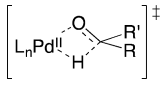

Figure 7. Four-membered transition states for β-hydride elimination from a Pd^{II}-alkoxide.

CONCLUSIONS

The study described herein resolves long-standing questions about the mechanism of Cu/TEMPO-catalyzed alcohol oxidation by reconciling an array of experimental data that have provided the basis for the different mechanistic proposals. Specifically, a concerted two-electron alcohol oxidation pathway involving a closed-shell η^1–nitroxyl–Cu adduct, identified by DFT computational methods, is shown to be favored over intramolecular and intermolecular homolytic mechanisms. It further rationalizes experimentally determined catalytic laws and accounts for the steric and kinetic effects of alcohol oxidations that employ TEMPO and ABNO cocatalysts. Cu/TEMPO is commonly described as a functional mimic of galactose oxidase, but the mechanistic conclusions highlight important distinctions between the two systems in light of the strong evidence for radical intermediates in the enzymatic reaction.

ASSOCIATED CONTENT

Supporting Information

Experimental details and characterization data for radical-probe oxidation reactions and computational details and atomic coordinates and energies for all computed structures. This material is available free of charge via the Internet at http://pubs.acs.org.

AUTHOR INFORMATION

Corresponding Author

stahl@chem.wisc.edu

Notes

The authors declare no competing financial interest.

ACKNOWLEDGMENTS

We are grateful to the DOE for financial support of this work (DE-FG02-05ER15690). The NSF provided partial support for the computational resources (CHE-0840494) and NMR instrumentation (NSF CHE-1048642 and NSF CHE-0342998) used in this work.

REFERENCES

(1) For reviews, see: (a) Sheldon, R. A.; Arends, I. W. C. E. *Adv. Synth. Catal.* **2004**, *346*, 1051–1071. (b) Cao, Q.; Dornan, L. M.; Rogan, L.; Hughes, N. L.; Muldoon, M. L. *Chem. Commun.* **2014**, *50*, 4524–4543. (c) Ryland, B. L.; Stahl, S. S. *Angew. Chem., Int. Ed.*, **2014**, Early View. DOI: 10.1002/anie.201403110.

(2) (a) Hoover, J. M.; Stahl, S. S. *J. Am. Chem. Soc.* **2011**, *133*, 16901–16910. (b) Hoover, J. M.; Steves, J. E.; Stahl, S. S. *Nat. Protoc.* **2012**, *7*, 1161–1166. (c) Hoover, J. M.; Stahl, S. S. *Org. Synth.* **2013**, *90*, 240–250.

(3) For discussion of related catalyst systems, see the reviews in ref 1 and the following leading references: (a) Semmelhack, M. F.; Schmid, C. R.; Cortés, D. A.; Chou, C. S. *J. Am. Chem. Soc.* **1984**, *106*, 3374–3376. (b) Gamez, P.; Arends, I. W. C. E.; Sheldon, R. A.; Reedijk, J. *Adv. Synth. Catal.* **2004**, *346*, 805–811. (c) Kumpulainen, E. T. T.; Koskinen, A. M. P. *Chem.—Eur. J.* **2009**, *15*, 10901–10911.

(4) Steves, J. E.; Stahl, S. S. *J. Am. Chem. Soc.* **2013**, *135*, 15742–15745.

(5) For discussion of related catalyst systems, see the review in ref 1 and the following leading references: (a) Sasano, Y.; Nagasawa, S.; Yamazaki, M.; Shibuya, M.; Park, J.; Iwabuchi, Y. *Angew. Chem., Int. Ed.* **2014**, *53*, 3236–3240. (b) Rogan, L.; Hughes, N. L.; Cao, Q.; Dornan, L. M.; Muldoon, M. J. *Catal. Sci. Technol.* **2014**, *4*, 1720–1725.

(6) For a recent comprehensive reviews, see: Bobbitt, J. M.; Brückner, C.; Merbouh, N. *Org. React. (Hoboken, NJ, U.S.)* **2010**, *74*, 103–424.

(7) (a) Hoover, J. M.; Ryland, B. L.; Stahl, S. S. *J. Am. Chem. Soc.* **2013**, *135*, 2357–2367. (b) Hoover, J. M.; Ryland, B. L.; Stahl, S. S. *ACS Catal.* **2013**, *3*, 2599–2605.

(8) (a) Dijksman, A.; Arends, I. W. C. E.; Sheldon, R. A. *Org. Biomol. Chem.* **2003**, *1*, 3232–3237. (b) Gamez, G.; Arends, I. W. C. E.; Reedijk, J.; Sheldon, R. A. *Chem. Commun.* **2003**, 2414–2415.

(9) Brackman, W.; Gaasbeek, C. *Recl. Trav. Chim. Pays-Bas* **1966**, *85*, 221−241.
(10) (a) Dickman, M. H.; Doedens, R. J. *Inorg. Chem.* **1981**, *20*, 2677−2681. (b) Porter, L. C.; Dickman, M. H.; Doedens, R. J. *Inorg. Chem.* **1986**, *25*, 678−684. (c) Caneschi, A.; Grand, A.; Laugier, J.; Rey, P.; Subra, R. *J. Am. Chem. Soc.* **1988**, *110*, 2307−2309. (d) Laugier, J.; Latour, J. M.; Caneschi, A.; Rey, P. *Inorg. Chem.* **1991**, *30*, 4474−4477.
(11) (a) Michel, C.; Belanzoni, P.; Gamez, P.; Reedijk, J.; Baerends, E. J. *Inorg. Chem.* **2009**, *48*, 11909−11920. (b) Belanzoni, P.; Michel, C.; Baerends, E. J. *Inorg. Chem.* **2011**, *50*, 11896−11904.
(12) Cheng, L.; Wang, J.; Wang, M.; Wu, Z. *Inorg. Chem.* **2010**, *49*, 9392−9399.
(13) Gamba, I.; Mutikainen, I.; Bouwman, E.; Reedijk, J.; Bonnet, S. *Eur. J. Inorg. Chem.* **2013**, 115−123.
(14) (a) Branchaud, B. P.; Montague-Smith, M. P.; Kosman, D. J.; McLaren, F. R. *J. Am. Chem. Soc.* **1993**, *115*, 798−800. (b) Wachter, R. M.; Branchaud, B. P. *J. Am. Chem. Soc.* **1996**, *118*, 2782−2789. (c) Wachter, R. M.; Montague-Smith, M. P.; Branchaud, B. P. *J. Am. Chem. Soc.* **1997**, *119*, 7743−7749. (d) Turner, B. E.; Branchaud, B. P. *Bioorg. Med. Chem. Lett.* **1999**, *9*, 3341−3346. (e) Himo, F.; Eriksson, L. A.; Maseras, F.; Siegbahn, P. E. M. *J. Am. Chem. Soc.* **2000**, *122*, 8031−8036. (f) Whittaker, M. M.; Whittaker, J. W. *Biochemistry* **2001**, *40*, 7140−7148. (g) Branchaud, B. P.; Turner, B. E. *Methods Enzymol.* **2002**, *354*, 415−425.
(15) Rocek, J.; Radkowsky, A. E. *J. Am. Chem. Soc.* **1968**, *90*, 2986−2988.
(16) Rocek, J.; Aylward, D. E. *J. Am. Chem. Soc.* **1975**, *97*, 5452−5456.
(17) (a) Pestovsky, O.; Bakac, A. *J. Am. Chem. Soc.* **2004**, *126*, 13757−13764. (b) Beach, E. S.; Malecky, R. T.; Gil, R. R.; Horwitz, C. P.; Collins, T. J. *Catal. Sci. Technol.* **2011**, *1*, 437−443. (c) Lee, D. G.; Gai, H. *Can. J. Chem.* **1993**, *71*, 1394−1400.
(18) Meyer, K.; Rocek, J. *J. Am. Chem. Soc.* **1972**, *94*, 1209−1214.
(19) Whitesides, G. M.; Sadowski, J. S.; Lilburn, J. *J. Am. Chem. Soc.* **1974**, *96*, 2829−2835.
(20) Lee, D. G.; Chen, T. *J. Org. Chem.* **1991**, *56*, 5341−5345.
(21) Lee, D. G.; Spitzer, U. A.; Cleland, J.; Olson, M. E. *Can. J. Chem.* **1976**, *54*, 2124−2126.
(22) For a study of the rearrangement of the parent cyclopropylcarbinol radical species, see: Davies, A. G.; Muggleton, B. *J. Chem. Soc., Perkin Trans. 2* **1976**, 502−510.
(23) For examples of the use of this as a probe for synthetic alcohol oxidation systems, see, e.g., (a) Kretzschmar, I.; Levinson, J. A.; Friend, C. M. *J. Am. Chem. Soc.* **2000**, *122*, 12395−12396. (b) Markó, I. E.; Gautier, A.; Mutonkole, J.-L.; Dumeunier, R.; Ates, A.; Urch, C. J.; Brown, S. M. *J. Organomet. Chem.* **2001**, *624*, 344−347.
(24) Tanko, J. M.; Drumright, R. E. *J. Am. Chem. Soc.* **1992**, *114*, 1844−1854.
(25) Astolfi, P.; Brandi, P.; Galli, C.; Gentili, P.; Gerini, M. F.; Greci, L.; Lanzalunga, O. *New J. Chem.* **2005**, *29*, 1308−1317.
(26) Tanko, J. M.; Phillips, J. P. *J. Am. Chem. Soc.* **1999**, *121*, 6078−6079.
(27) The estimated experimental barriers are obtained from the initial rates measured under the reaction conditions reported in ref 7a, adjusted to account for standard states for all reagents.
(28) See Supporting Information for details.
(29) For pK_a of benzyl alcohols see: Bordwell, F. G.; Liu, W.-Z. *J. Am. Chem. Soc.* **1996**, *118*, 8777−8781.
(30) Olmstead, W. N.; Margolin, Z.; Bordwell, F. G. *J. Org. Chem.* **1980**, *45*, 3295−3299.
(31) Lauber, M. B.; Stahl, S. S. *ACS Catal.* **2013**, *3*, 2612−2616.
(32) Numerous TEMPO complexes with metals other than Cu have been reported. For leading references, see: (a) Dickman, M. H.; Doedens, R. J. *Inorg. Chem.* **1982**, *21*, 682−684. (b) Jaitner, P.; Huber, W.; Gieren, A.; Betz, H. *J. Organomet. Chem.* **1986**, *311*, 379−385. (c) Mahanthappa, M. K.; Huang, K.-W.; Cole, A. P.; Waymouth, R. M. *Chem. Commun.* **2002**, 502−503. (d) Isrow, D.; Captain, B. *Inorg. Chem.* **2011**, *50*, 5864−5866. (e) Smith, J. M.; Mayberry, D. E.; Margarit, C. G.; Sutter, J.; Wang, H.; Meyer, K.; Bontchev, R. P. *J. Am. Chem. Soc.* **2012**, *134*, 6516−6519. (f) Scepaniak, J. J.; Wright, A. M.; Lewis, R. A.; Wu, G.; Hayton, T. W. *J. Am. Chem. Soc.* **2012**, *134*, 19350−19353. (g) Lomont, J. P.; Nguyen, S. C.; Harris, C. B. *J. Am. Chem. Soc.* **2013**, *135*, 11266−11273. (h) Wright, A. M.; Zaman, H. T.; Wu, G.; Hayton, T. W. *Inorg. Chem.* **2013**, *52*, 3207−3216.
(33) de Graauw, C. F.; Peters, J. A.; van Bekkum, H.; Huskens, J. *Synthesis* **1994**, 1007−1017.
(34) For representative reviews, see: (a) Sheldon, R. A.; Arends, I. W. C. E.; ten Brink, G.-J.; Dijksman, A. *Acc. Chem. Res.* **2002**, *35*, 774−781. (b) Stahl, S. S. *Angew. Chem., Int. Ed.* **2004**, *43*, 3400−3420. (c) Schultz, M. J.; Sigman, M. S. *Tetrahedron* **2006**, *62*, 8227−8241.
(35) For a comparison of homogeneous Pd and Cu/TEMPO catalyst systems under continuous flow conditions, see: (a) Ye, X.; Johnson, M. D.; Diao, T.; Yates, M. H.; Stahl, S. S. *Green Chem.* **2010**, *12*, 1180−1186. (b) Greene, J. F.; Hoover, J. M.; Mannel, D. S.; Root, T. W.; Stahl, S. S. *Org. Process Res. Dev.* **2013**, *17*, 1247−1251.